JOURNAL OF THE AMERICAN CHEMICAL SOCIETY

Article

Ionic Thermotropic Liquid Crystal Dendrimers

Rafael Martn-Rapn, Mercedes Marcos, Ana Omenat, Joaqun Barber, Pilar Romero, and Jos L. Serrano

J. Am. Chem. Soc., **2005**, 127 (20), 7397-7403• DOI: 10.1021/ja042264h • Publication Date (Web): 03 May 2005

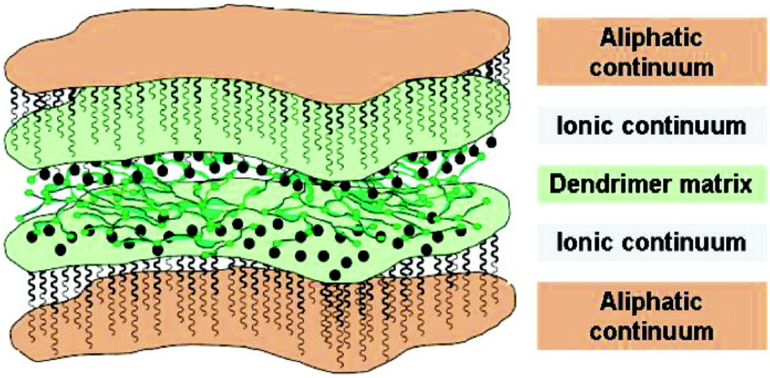

ACS Publications
High quality. High impact.

Journal of the American Chemical Society is published by the American Chemical Society. 1155 Sixteenth Street N.W., Washington, DC 20036

J|A|C|S
ARTICLES

Ionic Thermotropic Liquid Crystal Dendrimers

Rafael Martín-Rapún, Mercedes Marcos, Ana Omenat, Joaquín Barberá,
Pilar Romero, and José L. Serrano*

*Contribution from the Dpto. de Química Orgánica, Instituto de Ciencia de Materiales de
Aragón, Universidad de Zaragoza-CSIC, 50009 Zaragoza, Spain*

Received December 23, 2004; Revised Manuscript Received March 30, 2005; E-mail: joseluis@unizar.es

---

Abstract: The synthesis and characterization of two families of ionic liquid crystal dendrimers consisting of the ammonium salts of the commercially available poly(amidoamine) ($G = 0-5$) and poly(propylene imine) ($G = 1-5$) dendrimers and three long-chain carboxylic acids are reported. The liquid crystalline behavior was investigated by means of differential scanning calorimetry, polarizing light optical microscopy, and X-ray diffractometry. The thermal stability of the ionic materials was further studied by NMR. Most of the dendrimers show lamellar mesomorphism, and two of them exhibit columnar mesomorphism. On the basis of the experimental results, we propose models both at the molecular level and in the mesophase for all the materials.

Introduction

Liquid crystal (LC) dendrimers constitute one of the most significant and original matters of the liquid-phase-occurring phenomena, studied in the field of supramolecular chemistry.[1,2] Most of the LC dendrimers reported up to date are prepared by one of the two following general synthetic approaches: (a) the formation of macrostructures with a regular structural growth[3−9] by successive introduction of the mesogenic units within the branches in each dendrimer generation[5,10−12] or (b) the functionalization of a pre-existing dendrimer by the covalent linkage of the mesogenic units to its peripheral functional groups (amino, carboxylate, silane, etc.). In this way, it is possible to obtain dendritic architectures that display LC properties by the introduction of rodlike[1,13−22] or disklike[1,23] mesogenic units at the periphery of the original dendrimer, thus forming a LC shell around the central dendritic nucleus. The formation of a LC phase as a result of the molecular arrangement at the supramolecular level is determined by the microsegregation of the three molecular regions with very diverse characteristics which are present in this type of LC dendrimers (central dendrimeric core, mesogenic units and terminal flexible chains), in such a way that the molecule tends to adopt the thermodynamically most stable conformation.[13,16,24,25] In the case of lamellar mesophases, the proposed molecular model leads to consider the molecules as super-rods that would be ordered parallel to each other, promoting a smectic mesophase. For the columnar mesophases, however, a model in which the molecule adopts a radial *disklike* conformation has been postulated.[25] The mesophase is formed as a result of the packing of these molecules within columns. In all these cases, the LC materials are constituted by covalent neutral molecules. In the field of LC, however, it is well known that ionic amphiphiles, such as protonated amines, carboxylates, sulfonates, pyridinium, and quaternary phosphonium salts, self-assemble in solvents to form a variety of lyotropic and/or thermotropic LC.[26−31] As it can

---

(1) Ponomarenko, S. A.; Boiko, N. I.; Shibaev, V. P. *Polym. Sci., Ser. C* **2001**, *43*, 1.
(2) Steed, J. W.; Atwood, J. L. *Supramolecular Chemistry*; John Wiley & Sons, Ltd.: Chichester, 2000.
(3) Kim, Y. H. *J. Am. Chem. Soc.* **1992**, *114*, 4947.
(4) Percec, V.; Kawasumi, M. *Polym. Prepr.* **1992**, *33*, 221.
(5) Percec, V.; Chu, P. V.; Kawasumi, M.; Toward, M. *Macromolecules* **1994**, *27*, 4441.
(6) Percec, V. *Pure Appl. Chem.* **1995**, *67*, 2031.
(7) Plesnivy, T.; Ringsdorf, H.; Schuhmacher, P.; Nüutz, U.; Diele, S. *Liq. Cryst.* **1995**, *18*, 185.
(8) Gehringer, L.; Guillon, D.; Donnio, B. *Macromolecules* **2003**, *36*, 5593.
(9) Gehringer, L.; Bourgogne, C.; Guillon, D.; Donnio, B. *J. Am. Chem. Soc.* **2004**, *126*, 3856.
(10) Percec, V.; Kawasumi, M. *Macromolecules* **1992**, *25*, 3843.
(11) Bauer, S.; Fischer, H.; Ringsdorf, H. *Angew. Chem., Int. Ed. Engl.* **1993**, *32*, 1589.
(12) Hudson, S. D.; Jung, H. T.; Percec, V.; Cho, D. W.; Johansson, G.; Ungar, G.; Balagurusamy, U. S. K. *Science* **1997**, *278*, 449.
(13) Ponomarenko, S. A.; Rebrov, E. A.; Brobonsky, A. Y.; Boiko, N. I.; Muzafarov, A. M.; Shibaev, V. P. *Liq. Cryst.* **1996**, *21*, 1.
(14) Ponomarenko, S. A.; Boiko, N. I.; Shibaev, V. P.; Richardson, R. M.; Whitehouse, I. J.; Rebrov, E. A.; Muzafarov, A. M. *Macromolecules* **2000**, *33*, 5549.
(15) Lorenz, K.; Hölter, D.; Mühlhaupt, R.; Frey, H. *Adv. Mater.* **1996**, *8*, 414.
(16) Baars, M. W. P. L.; Söntjens, S. H.; Fischer, H.; Peerlings, H. W. I.; Meijer, E. W. *Chem.−Eur. J.* **1998**, *4*, 2456.
(17) Barberá, J.; Marcos, M.; Serrano, J. L. *Chem.−Eur. J.* **1999**, *5*, 1834.
(18) Marcos, M.; Giménez, R.; Serrano, J. L.; Donnio, B.; Heinrich, B.; Guillon, D. *Chem.−Eur. J.* **2001**, *7*, 1006.
(19) Donnio, B.; Barberá, J.; Giménez, R.; Guillon, D.; Marcos, M.; Serrano, J. L. *Macromolecules* **2002**, *35*, 370.
(20) Barberá, J.; Giménez, R.; Marcos, M.; Serrano, J. L. *Liq. Cryst.* **2002**, *29*, 309.
(21) Serrano, J. L.; Marcos, M.; Martín, R.; González, M.; Barberá, J. *Chem. Mater.* **2003**, *15*, 3866.
(22) Rueff, J.-M.; Barberá, J.; Donnio, B.; Guillon, D.; Marcos, M.; Serrano, J. L. *Macromolecules* **2003**, *36*, 8368.
(23) McKenna, M. D.; Barberá, J.; Marcos, M.; Serrano, J. L. *J. Am. Chem. Soc.* **2005**, *127*, 619.
(24) Barberá, J.; Donnio, B.; Giménez, R.; Guillon, D.; Marcos, M.; Omenat, A.; Serrano, J. L. *J. Mater. Chem.* **2001**, *11*, 2808.
(25) Marcos, M.; Omenat, A.; Serrano, J. L. *CR Chim.* **2003**, *6*, 947.
(26) Skoulios, A.; Guillon, D. *Mol. Cryst. Liq. Cryst.* **1988**, *165*, 317.
(27) Paleos, C. M. *Mol. Cryst. Liq. Cryst.* **1994**, *243*, 159.
(28) Dreja, M.; Gramberg, S.; Tieke, B. *Chem. Commun.* **1998**, 1371.
(29) Ohta, K.; Sugiyama, T.; Nogami, T. *J. Mater. Chem.* **2000**, *10*, 613.
(30) Nikovoura, A.; Tsiourvas, D.; Arkas, M.; Sideratou, Z.; Paleos, C. M. *Liq. Cryst.* **2002**, *29*, 1547.
(31) Ujiie, S.; Takagi, S.; Sato, M. *High Perform. Polym.* **1998**, *10*, 139.

10.1021/ja042264h CCC: $30.25

be easily understood, the driving force to the formation of mesophases is, in this case, the segregation of the lipophilic and hydrophilic moieties of the molecules, which gives rise to ordered supramolecular structures. Therefore, the presence of anisotropic mesogenic units in the structure of a molecule is not anymore necessary to obtain a material with liquid crystal properties. The translation of this idea to the field of the dendrimers is immediate if we take into account that the surface of amino-terminated dendrimers can be modified with long-chain carboxylic acids, as already reported by several authors.[32−35] Crooks et al.[32] described a simple, noncovalent way of converting the hydrophilic dendrimer periphery to hydrophobic by the formation of ion pairs between the carboxylate group of a fatty acid and the terminal amino group of the poly(amidoamine) (PAMAM) dendrimers. These materials were prepared and investigated for their use in catalytic applications. Ramzi et al.[33] have also modified the end groups of poly(propylene imine) (PPI) dendrimers (G3 and G5) with octadecanoic and octadecanoic-d_{35} acids. Tomalia et al.[34] reported on the lyotropic LC behavior of a material resulting from the ionic interaction of the G3 PPI dendrimer and octanoic acid. In this case, the dendrimer served as solvent in a lamellar lyotropic liquid crystal. Recently, Stiriba et al.[35] have described the complexes formed by hyperbranched polyethylenimine (PEI) and fatty acids, which give rise to supramolecular inverted micellar structures that are able to irreversibly transfer water-soluble guest molecules into organic solvents. In 1995, Lattermann et al.[36] described the first member of a series of ionic columnar dendromesogens. The synthesis and liquid crystal properties of PAMAM dendrimer−fluorosurfactant complexes, which change of structure from planar to spherical depending on the generation (from $G = 0-4$) were reported by Faul et al.[37]

Tsiourvas et al.[38] have described the thermotropic liquid crystalline behavior of a family of ionic dendrimers derived from the protonation of PPI with a cholesterol-based carboxylic acid. These LC dendrimers show smectic C* and smectic A mesophases. In this case, however, still a mesogenic unit, namely, the cholesteryl moiety, is incorporated onto the periphery of the PPI dendrimer, although via an ionic interaction.

At the same time that the present work was in progress, Ujiie et al.[39] have prepared the ionic LC dendrimers derived from the generation 3.0 PAMAM dendrimer and stearic, palmitic, and myristic acids. In all the three cases, the dendrimers show a smectic A mesophase.

It is also noteworthy that the incorporation of an alkanoic acid onto the periphery of PPI dendrimers via a covalent amide bond, namely, by reaction of the amino terminal groups with the corresponding acid chloride, afford nonmesomorphic materials.[40] Thus, it can be deduced that the ionic interaction between the dendrimer peripheral quaternary ammonium salts and the carboxylate groups of the long-chain acids is decisive to the generation of a mesomorphic ordered structure.

Scheme 1. Synthetic Route to Ionic Dendrimers

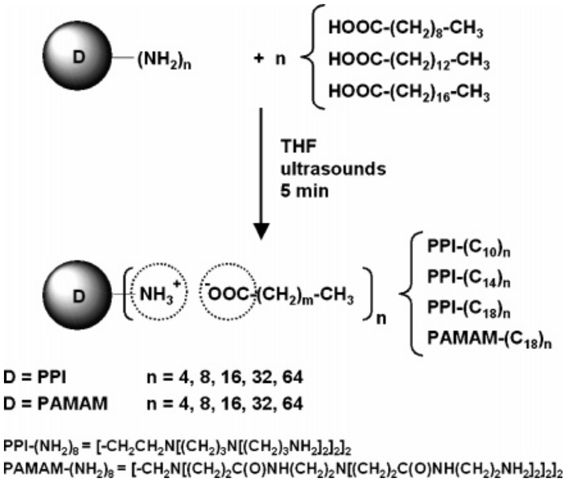

In this work, we describe the spontaneous assembly of the carboxylic acids ($HOOC(CH_2)_mCH_3$, with $m = 8$, 12, and 16) onto the surface of amino-terminated PPI ($PPI-(NH_2)_n$, with $n = 4$, 8, 16, 32, and 64) and the stearic acid ($m = 16$) onto the poly(amidoamine) ($PAMAM-(NH_2)_n$, with $n = 4$, 8, 16, 32, 64, and 128) (See Scheme 1). The liquid crystalline properties of these materials have been thoroughly investigated by means of polarizing optical microscopy (POM), differential scanning calorimetry (DSC), and X-ray diffraction (XRD). On the basis of the results obtained, especially by XRD, a molecular model in the mesophase can be proposed. Moreover, the thermal study of the materials affords significant data on their stability. The transformations suffered by the dendrimers on the successive heating and cooling cycles as well as the protonation of the primary and the tertiary amine groups of the dendrimers have been investigated by $^1H-^1H$−COSY and $^1H-^{13}C$−HSQC NMR experiments.

Results and Discussion

Synthesis and Characterization. The synthesis of the ionic dendrimers is outlined in Scheme 1. Amine-terminated PAMAM or PPI dendrimer was added to a solution of the corresponding alkanoic acid in dry tetrahydrofuran (THF), in approximately 1:1 (primary amine groups: carboxylic acid groups) stoichiometry, following the method described by R. M. Crooks et al.[32]

Fourier Transform (FT) IR Study. The formation of the ammonium alkanoate salts was confirmed by FT IR measurements. In every case, the carbonyl stretching absorption band at about 1710 cm^{-1} disappeared, while two bands at ca. 1555 and 1405 cm^{-1} corresponding, respectively, to the asymmetric and symmetric stretching modes of the carboxylate groups appeared (Figure 1).

The main IR data for PAMAM and PPI ionic dendrimers are gathered in the tables available in the Supporting Information.

Thermal Study. The phase behavior of the ionic dendrimers was investigated by POM and DSC. The transition temperatures and enthalpies obtained from the DSC thermograms are gathered

---

[32] Chechik, V.; Zhao, M.; Crooks, R. M. *J. Am. Chem. Soc.* **1999**, *121*, 4910.
[33] Ramzi, A.; Bauer, B. J.; Scherrenberg, R.; Froehling, P.; Joosten, J.; Amis, E. J. *Macromolecules* **1999**, *32*, 4983.
[34] Friberg, S. E.; Podzimek, M.; Tomalia, D. A.; Hedstrand, D. M. *Mol. Cryst. Liq. Cryst.* **1988**, *164*, 157.
[35] Chen, Y.; Shen, Z.; Frey, H.; Pérez-Prieto, J.; Stiriba, S.-E. *Chem. Commun.* **2005**, *6*, 755.
[36] Cameron, J. H.; Facher, A.; Stebani, G.; Lattermann, G. *Adv. Mater.* **1995**, *7*, 578.
[37] Faul, C. F. J.; Antonietti, M.; Hentze, M. P.; Smarly, B. *Colloids Surfaces, Physicochem. Eng. Asp.* **2003**, *212*, 115.
[38] Tsiourvas, D.; Felekis, T.; Sideratou, Z.; Paleos, C. M. *Liq. Cryst.* **2004**, *31*, 739.
[39] Ujiie, S.; Yano, Y.; Mori, A. *Mol. Cryst. Liq. Cryst.* **2004**, *411*, 483.
[40] Stevelmans, S.; van Hest, J. C. M.; Jansen, J. F. G. A.; van Boxtel, D. A. F. J.; de Brabander-van den Berg, E. M. M.; Meijer, E. W. *J. Am. Chem. Soc.* **1996**, *118*, 7398.

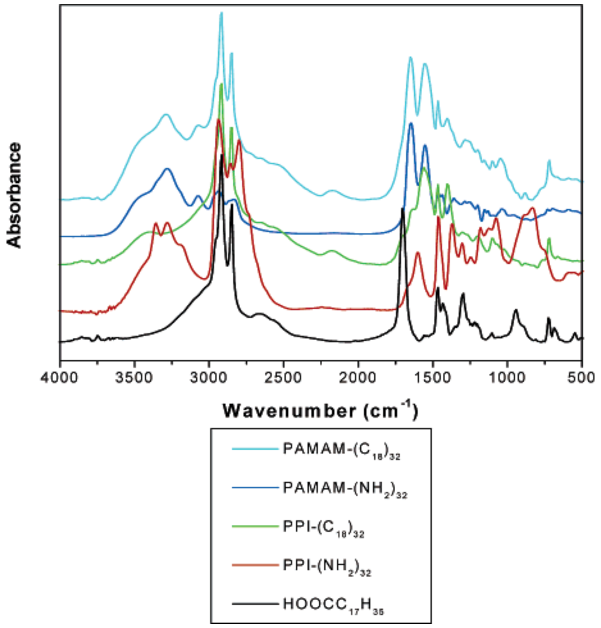

Figure 1. FT IR spectra of the stearic acid (black), PPI$-(NH_2)_{32}$ dendrimer (red), PPI-stearate dendrimer (green), PAMAM$-(NH_2)_{32}$ dendrimer (blue), and PAMAM$-$stearate dendrimer (cyan).

Table 1. Transition Temperatures and Enthalpies as Determined by DSC[a] of PAMAM Ionic Dendrimers

dendrimer	scan	transitions (°C), (ΔH (kJ mol^{-1})) heating process[a]
PAMAM$-(C_{18})_4$	1st	C_1 39 (109.7) C_2 48 SmA 135 (7.1) I
	5th	C_1 34 (22.0) C_2 55 (52.2) SmA 99 (15.0) I
PAMAM$-(C_{18})_8$	1st	C_1 58 C_2 67 (571.9) SmA 151 (15.5) I
	5th	C_1 57 C_2 71 (454.9) SmA 130 (13.4) I
PAMAM$-(C_{18})_{16}$	1st	C_1 61 C_2 71 (933.1) SmA 148 (16.6) I
	5th	g 33 C_1 56 (351.4) C_2 63 (239.0) SmA 126 (19.5) I
PAMAM$-(C_{18})_{32}$	1st	C_1 41 (79.6) C_2 63 (727.6) SmA 138 (24.9) I
	5th	g 16 C 50 C 53 (916.2) SmA 130 (25.9) I
PAMAM$-(C_{18})_{64}$	1st	C_1 49 (707.8) C_2 69 (1931.7) SmA 151 (72.1) I
	5th	g 22 C_1 54 (1032.3) C_2 62 (1351.7) SmA 133 (71.7) I
PAMAM$-(C_{18})_{128}$	1st	C_1 52 (1113.0) C_2 70 (3913.1) SmA 156 (114.2) I
	5th	g 19 C_1 56 (1835.9) C_2 63 (2359.7) SmA 140 (156.6) I

[a] C = crystal, g = glass, SmA = smectic A mesophase, I = isotropic liquid.

Table 2. Transition Temperatures and Enthalpies as Determined by DSC[a] of PPI Ionic Dendrimers (2nd Scan)

dendrimer	transitions (°C), (ΔH (kJ mol^{-1})) heating process[a]
PPI$-(C_{18})_4$	C_1 60 (236.0) C_2 67 (74.7) SmA 116 (6.7) I
PPI$-(C_{18})_8$	C_1 55 (229.1) SmA 134 (21.4) I
PPI$-(C_{18})_{16}$	C_1 56 (326.6) SmA 131 (15.0) I
PPI$-(C_{18})_{32}$	C_1 48 (773.3) SmA 127 (50.8) I
PPI$-(C_{18})_{64}$	C_1 51 (2007.2) C_2 68 Col_{tet} 102 (91.6) I
PPI$-(C_{14})_4$	C_1 27 (134.0) SmA 116 (9.7) I
PPI$-(C_{14})_8$	C_1 28 (256.1) SmA 125 (16.1) I
PPI$-(C_{14})_{16}$	C_1 24 (303.9) C_2 34 (65.0) SmA 127[b] I
PPI$-(C_{14})_{32}$	C_1 11 (681.9) SmA 73 (55.1) I
PPI$-(C_{14})_{64}$	C_1 5 (1240.4) Col_h 78 (13.7) I
PPI$-(C_{10})_4$	SmA 100 (7.6) I
PPI$-(C_{10})_8$	SmA 103 (12.9) I
PPI$-(C_{10})_{16}$	SmA 34 (17.9) I

[a] C = crystal, g = glass, SmA = smectic A mesophase, Col_h = columnar hexagonal mesophase, Col_{tet} = columnar tetragonal mesophase, I = isotropic liquid. [b] Temperatures determined by polarized optical microscopy.

in Table 1 (PAMAM, 1st and 5th heating and cooling scans) and Table 2 (PPI, 2nd heating and cooling scans). In general, the transition temperatures are dendrimer-generation independent but significantly influenced by the alkanoic acid length and the dendrimer matrix considered.

Most of the ionic dendrimers under study show a lamellar mesophase, namely, a smectic A (SmA) phase. PPI$-(C_{10})_n$ ionic dendrimers exhibit lamellar mesophases in the first three generations. PPI$-(C_{14})_n$ and PPI$-(C_{18})_n$ dendrimers show a lamellar mesophase when $n = 4$, 8, 16, and 32 and a columnar one when $n = 64$. The occurrence of this type of mesomorphism can be explained by the surface congestion of the peripheral amino groups in the fifth generation of the PPI dendrimer. In contrast, PAMAM dendrimers show no columnar mesomorphism, even for the generation containing 128 terminal amino groups. The larger volume of the PAMAM dendritic architecture with respect to the PPI one prevents the steric hindrance of the primary amino groups on the surface. This fact evidences once again the flexibility and plasticity of the dendrimeric core, which adopts the most appropriate conformation to favor the interaction of the units responsible of the mesomorphic organization.[24,25]

When comparing the dendrimers in the PPI series, it can be seen that an increase in the length of the alkanoate moiety causes an increase of the transition temperature since a more ordered structure is favored. Accordingly, the PPI-decanoate salts are liquid crystals below room temperature, whereas the PPI$-$octadecanoate derivatives melt at temperatures higher than 50 °C.

As it is usually observed, the PAMAM-derived dendrimers show higher transition temperatures than their PPI homologues, probably due to the existence of hydrogen bonds within their structure.

With reference to the thermal stability of these materials, the successive heating scans of the ionic dendrimers promote a progressive decrease in the clearing point of the sample under study as it is schematized in Figure 2 for the PAMAM-derived dendrimers. However, after the fifth thermal cycle, the transition temperatures remain almost constant. A similar but less pronounced behavior is observed in the case of the PPI-derived dendrimers with clearing points higher than ca. 100 °C. Those dendrimers with lower transition temperatures afford reproducible DSC consecutive heating scans. Thus, it seems evident that the dendrimers suffer some kind of chemical transformation which is temperature dependent and results in a modification of the transition temperatures of the materials. For this reason, we give the thermal data of the dendrimers for the first and fifth heating scans in the case of the PAMAM derivatives and after the second heating scan for the PPI ones in Tables 1 and 2, respectively.

The thermogravimetric analysis of the dendrimers show that these materials are thermally stable up to ca. 160 °C. No significant loss of weight occurs below this temperature in the experiment conditions.

NMR Study. To understand the cause of this behavior, the dendrimers were studied by several NMR techniques, such as one-dimensional ^{1}H and ^{13}C NMR and two-dimensional ^{1}H$-$^{1}H COSY and ^{1}H$-$^{13}C HSQC NMR. Samples consisting in the corresponding dendrimer before and after successive heating cycles were dissolved in $CDCl_3$. The results obtained confirmed the formation of the salts and provided further structural information.

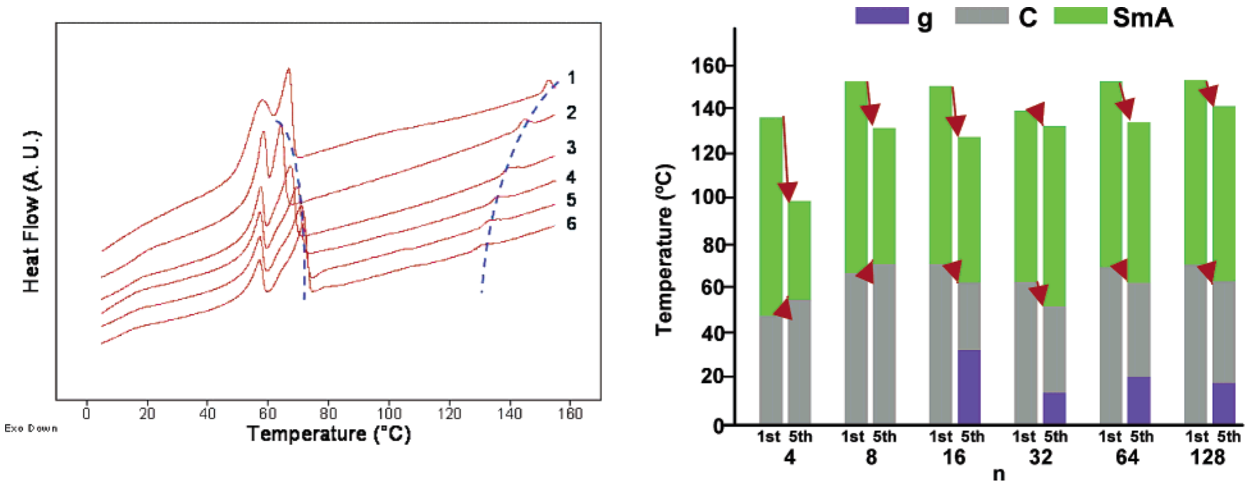

(a) (b)

Figure 2. (a) Evolution of the six consecutive DSC heating scans of PAMAM$-$(C$_{18}$)$_{16}$. (b) Schematic representation of the mesogenic behavior of PAMAM$-$(C$_{18}$)$_{n}$ dendrimers in the first and fifth heating scans.

The progressive decrease of the mesophase to isotropic liquid transition temperature after several DSC scans is clearly due to a change in the structure of the material. Two possibilities may be suggested a priori: the partial formation of amide bonds from the ammonium salts at high temperature or the migration of the carboxylic moieties inside the dendrimers resulting in the protonation of the inner tertiary amines. Both possibilities may be checked out by a careful analysis of the NMR spectra of samples consisting in the pristine ionic dendrimers and the thermally treated dendrimers. To obtain information about the assignment of the peaks corresponding to the protonation of the tertiary amines, the ionic dendrimers obtained from an excess of carboxylic acid, PAMAM$-$(C$_{18}$)$_{32}$ (1:2) and PPI$-$(C$_{18}$)$_{32}$ (1:2) were prepared and their NMR spectra were recorded. In the case of the PAMAM-derived dendrimer, a small percentage of protonated tertiary amines has been detected by the appearance of two signals at 3.18 (H^{a}) and 3.28 (H^{b}) ppm $-(\text{CO}-\text{CH}_2-\mathit{CH}_2{}^{a})_2-\text{NH}^{+}-\mathit{CH}_2{}^{b}-\text{CH}_2-\text{NH}-$, which are correlated via HSQC with two signals at 44.1 (C^{a}) and 39.4 ppm (C^{b}), respectively. For the PPI-derived dendrimer, the protonation of the tertiary amine groups occurs at a larger extent, which is confirmed by the appearance of a signal at 2.77 ppm (H^{c}) $-(-\mathit{CH}_2{}^{d}-\mathit{CH}_2{}^{c})_3-\text{NH}^{+}-$, which is correlated via HSQC with a signal at 51.4 ppm (C^{c}) and via COSY with signals at 1.76 ppm (H^{d}) and 22.7 ppm (C^{d})[38,41] (Figure 3a).

PAMAM$-$(C$_{18}$)$_{32}$, Untreated Sample. The NMR spectra obtained for this material reveal that the dendrimer ionic salts are formed by the protonation of the primary amine groups on the dendrimer surface, i.e., signals at 3.48 (H^{e}) and 3.04 ppm (H^{f}) and at 37.7 (C^{e}) and 39.3 ppm (C^{f}) $[-\mathit{CH}_2{}^{e}-\mathit{CH}_2{}^{f}-\text{NH}_3{}^{+}]$. No protonation of the tertiary amine groups is observed (Figure 3c). These data are in agreement with those reported by Tomalia et al.[42]

PAMAM$-$(C$_{18}$)$_{32}$, Treated Sample, after Seven Heating and Cooling Cycles. The NMR spectra of this sample show two new groups of signals with respect to the untreated sample, which are attributed to the formation of a certain percentage of amide bonds ($-$NH$-$CO$-$), namely, 20% relative to $-\text{CH}_2-\text{NH}_3{}^{+}$ groups, and to a small percentage, not accurately measurable, of protonated tertiary amine groups. The chemical shifts and correlations corresponding to these new sets of signals are the following: $-\mathit{CH}_2{}^{g}-\text{NH}-\mathit{C}^{h}\text{O}-$, 3.86 (H^{g}), 44.9 (C^{g}), and 174.6 ppm (C^{h}); $(\text{CO}-\text{CH}_2-\mathit{CH}_2{}^{i})_2-\text{NH}^{+}-\mathit{CH}_2{}^{j}-\text{CH}_2-\text{NH}-$, 3.18 (H^{i}), 3.28 (H^{j}), 44.1 (C^{i}), and 39.4 (C^{j}) (Figure 3d). The chemical transformations suffered by the ionic dendrimer after seven heating and cooling cycles involve both the formation of amide bonds at the dendrimer periphery and the protonation of inner tertiary amine groups.

PPI$-$(C$_{18}$)$_{32}$, Untreated Sample. The NMR spectra obtained for this material reveal that the dendrimer ionic salts are formed by the protonation of the primary amine groups on the dendrimer surface, i.e., signals at 2.97 (H^{k}) and at 38.6 ppm (C^{k}) $[-\mathit{CH}_2{}^{k}-\text{NH}_3{}^{+}]$.

PPI$-$(C$_{18}$)$_{32}$, Treated Sample, after Seven Heating and Cooling Cycles. In this case, a small percentage of amide bonds has been detected (ca. 8% relative to $-\text{CH}_2-\text{NH}_3{}^{+}$ groups), $[-\mathit{CH}_2{}^{l}-\text{NH}-\text{C}^{m}\text{O}-$, 3.20 (H^{l}), 37.1 (C^{l}), and 174.0 ppm (C^{m})] but no protonation of the tertiary amine groups is observed. (Figure 3b). This small percentage compared with the 20% observed for the PAMAM derivative may be attributed to the thermal decomposition of the latter compound.

Therefore, it can be concluded that the variation of the clearing points for the ionic dendrimers when subject to successive heating and cooling cycles is due to the partial formation of amide bonds between the terminal amino and carboxylate groups. That is especially the case for PAMAM-derived dendrimers, since higher temperatures are reached during their study than for PPI derivatives. In each heating cycle, the sample becomes impure by the presence of some amount of molecules with the alkanoyl moieties covalently bonded to the dendrimer matrix, which leads to a lowering of the transition temperatures.

XRD Study. The lamellar mesomorphism of most of the dendrimers was confirmed by powder XRD. The diffraction patterns of these materials consist of a diffuse halo in the wide-angle region, corresponding to the distance between the conformationally disordered alkyl chains, and a set of two maxima

---

(41) Baars, M. W. P. L.; Karlsson, A. J.; Sorokin, V.; de Waal, B. F. W.; Meijer, E. W. *Angew. Chem., Int. Ed.* **2000**, *39*, 4262.

(42) Tomalia, D. A.; Baker, H.; Dewald, J.; Hall, M.; Kallos, G.; Martin, S.; Roeck, J.; Ryder, J.; Smith, P. *Polym. J.* **1985**, *17*, 117.

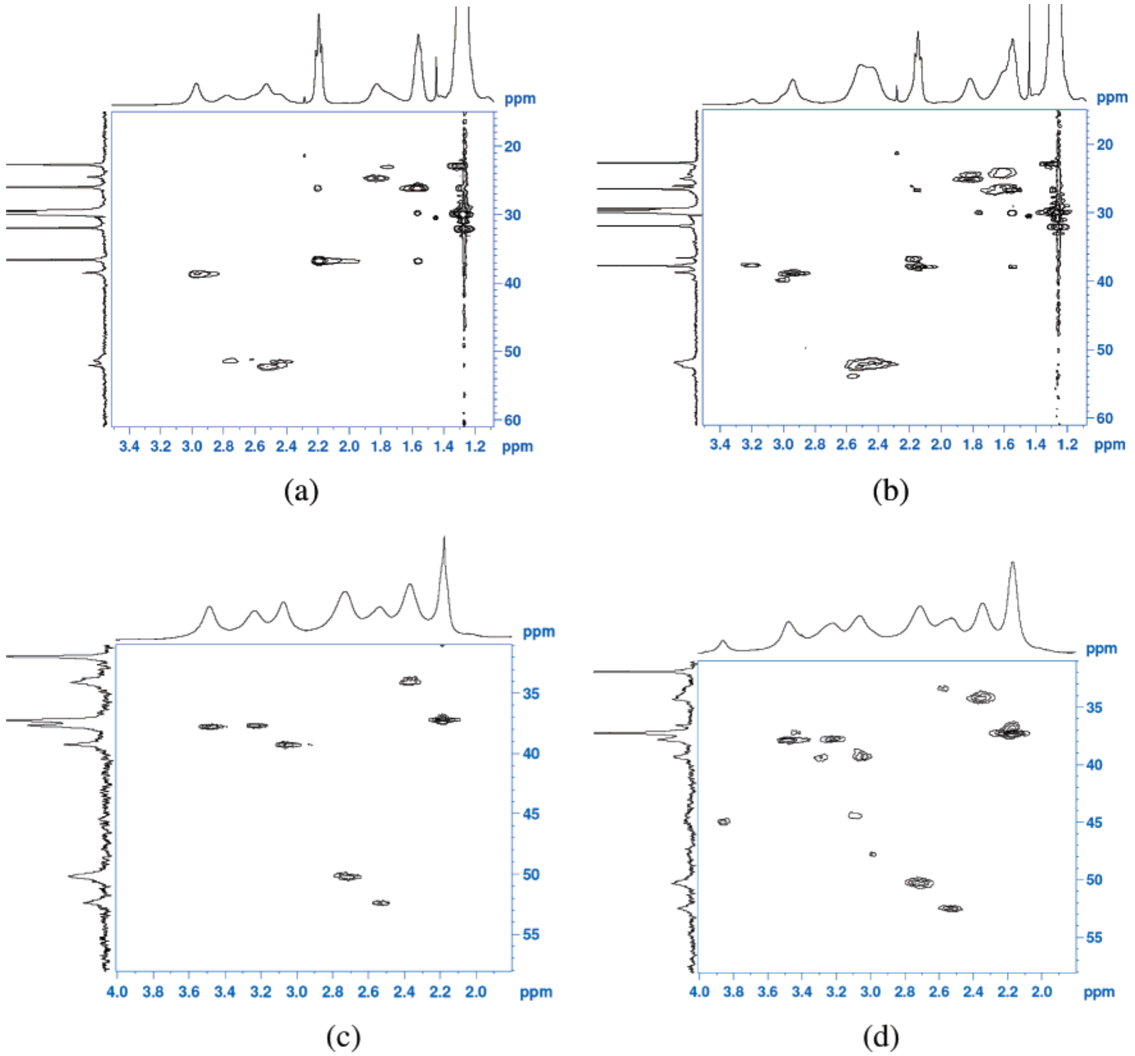

(a) (b)

(c) (d)

Figure 3. 2-D correlated ^{1}H and ^{13}C NMR spectra of the dendrimers (a) PPI−$(C_{18})_{32}$ (1:2), (b) PPI−$(C_{18})_{32}$, treated sample, after seven heating and cooling cycles, (c) PAMAM−$(C_{18})_{32}$, untreated sample, (d) PAMAM−$(C_{18})_{32}$, treated sample, after seven heating and cooling cycles.

Table 3. X-ray Data for the PAMAM−$(C_{18})_n$ Ionic Dendrimers

n	mesophase	*T*/°C	*d*/Å	heating cycles
4	SmA	75	36.1	1
8	SmA	75	41.4	1
16	SmA	75	45.3	1
32	SmA	75	44.3	1
64	SmA	75	46.4	1
128	SmA	75	49.5	1
4	SmA	71	42.3	6
8	SmA	71	46.4	6
16	SmA	71	44.3	6
32	SmA	71	46.4	6
64	SmA	71	45.3	6
128	SmA	71	44.7	6

Table 4. X-ray Data for the PPI−$(C_x)_n$ Ionic Dendrimers

n	x	mesophase	*T*/°C	d_1/Å	d_2/Å
4	10	SmA	57	23.5	
8	10	SmA	50	24.7	
16	10	SmA	50	23.1	
4	14	SmA	57	29.6	
8	14	SmA	50	30.4	
16	14	SmA	50	28.6	
32	14	SmA	41	27.0	
64	14	Col_h	50	28.7	16.8
4	18	SmA	77	34.8	
8	18	SmA	71	32.5	
16	18	SmA	77	34.2	
32	18	SmA	70	34.5	
64	18	Col_{tet}	84	36.1	25.0

in the low-angle region, which evidence a long range order. The spacings of these two maxima are in the reciprocal ratio 1:2. This pattern is consistent with a smectic A mesophase, as observed by POM. Tables 3 and 4 gather the values of the layer thickness in the SmA mesophase for all the dendrimers.

In the case of the PAMAM-derived dendrimers (Table 3), a progressive increase of *d* is observed when increasing the generation number of the dendrimer matrix in samples subject to one heating process. However, this trend vanishes when the samples are subject to several heating and cooling cycles, probably due to the dynamic behavior of the hydrogen bonds within the dendritic scaffold and to the flexibility of this scaffold in order to adapt itself to the volume-area ratio required for the accommodation of the alkyl carboxylate chains.

For the PPI-derived ionic dendrimers (Table 4), the layer thickness is independent of the generation number considered, and increases with the length of the alkanoate moiety.

The XRD patterns obtained from samples of PPI−$(C_{18})_{64}$ and PPI−$(C_{14})_{64}$ were not consistent with a lamellar mesomorphism

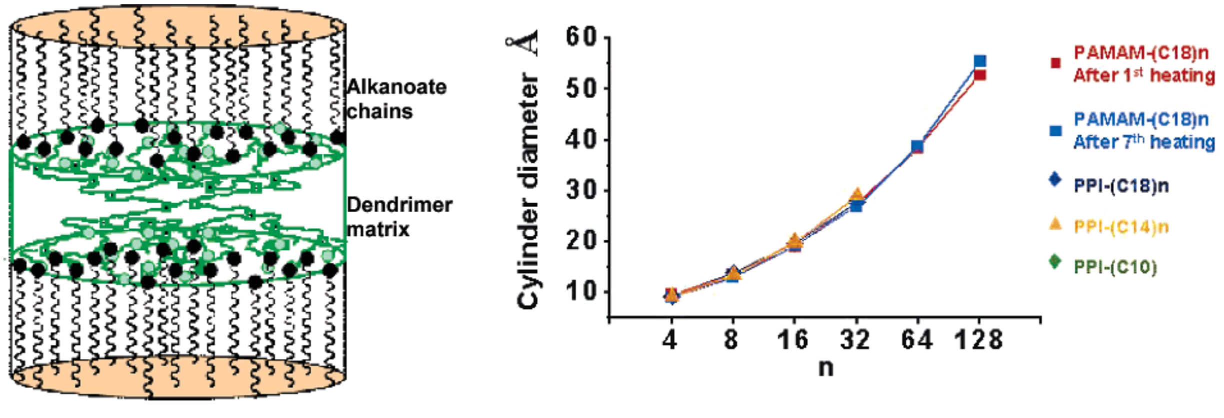

(a) (b)

Figure 4. (a) Molecular model for the ionic dendrimers with a lamellar mesomorphism. (b) Graphical representation of the cylinder diameter as a function of the generation number for all the dendrimers under study.

but with a columnar one. Both exhibit a diffuse maximum corresponding to a distance of ca. 4.5 Å between the conformationally disordered aliphatic chains. The hexagonal columnar phase of PPI$-$(C$_{14}$)$_{64}$ was assigned by the presence of a set of three sharp reflections in the reciprocal ratio 1:$\sqrt{3}$:$\sqrt{4}$ in the low-angle region of the patterns. For PPI$-$(C$_{18}$)$_{64}$, three reflections in the ratio 1:$\sqrt{2}$:$\sqrt{4}$ are observed. These results have led us to identify the mesophase as an unusual tetragonal columnar one, which has been previously reported for some phthalocyanine derivatives.[43−45]

On the basis of previous works on LC dendrimers,[16,17] we propose an ideal cylindrical model for the lamellar mesophases, in which the dendrimer matrix occupies the central section whereas the alkanoate chains extend up and down as shown in Figure 4a.

By use of the expressions described in the Supporting Information Appendix, we can make some theoretical calculations starting from the experimentally measured spacings *d* obtained by XRD and the values of molecular weight. In this way, we can estimate the values for the surface, diameter, and height of the cylinders constituted by the dendrimer as a whole and also those of the subcylinder occupied by the dendritic core itself. The results of these calculations show that the diameter of the cylinder increases with the generation number. The value of the diameter is similar in dendrimers of the same generation (PAMAM or PPI matrixes) and is independent of the chain length of the carboxylic acid. For example, the diameter of dendrimer PAMAM$-$(C$_{18}$)$_{16}$ is 19.1 Å and those of PPI$-$(C$_n$)$_{16}$ are 19.8 (n = 18), 19.9 (n = 14), and 20.2 Å (n = 10), respectively. In conclusion, the number of alkanoate chains influences the cylinder area, independently of the dendrimer matrix and the length of the carboxylic acid, as it is graphically represented in Figure 4b.

As a consequence of this molecular model, we propose a molecular organization in the SmA mesophase as shown in Figure 5.

PPI$-$(C$_{14}$)$_{64}$ and PPI$-$(C$_{18}$)$_{64}$ ionic dendrimers show columnar mesophases. In these cases, the molecular model consists of a cylinder with the dendrimer matrix occupying a central subcylinder and the carboxylate chains radially arranged, as represented in Figure 6.

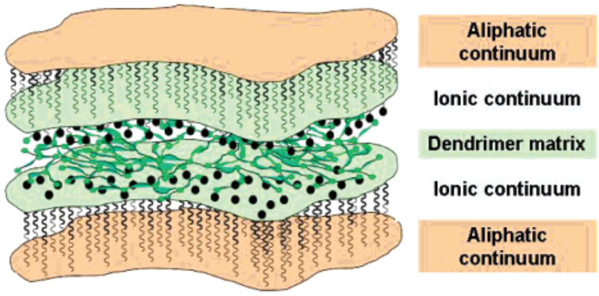

Figure 5. Schematic representation of the molecular organization in the SmA mesophase.

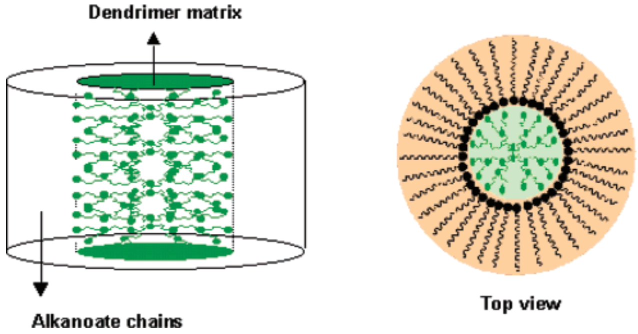

Figure 6. Molecular model for the ionic dendrimers with a columnar mesomorphism.

Depending on the length of the carboxylic acid and, therefore, the proportion of the aliphatic part with respect to the ionic and dendrimer matrix regions, two different two-dimensional lattices have been found. For the C$_{14}$ carboxylic acid, the columns arrange in a supramolecular hexagonal lattice, while for the C$_{18}$ carboxylic acid, a square lattice is proposed (Figure 7).

The supramolecular organizations obtained, both lamellar and columnar, the chemical nature of the segregated areas, as well as the ability of these dendrimer materials to afford oriented films and fibers allow us to envisage the possibility of obtaining interesting physical properties, such as ionic conductivity. The preparation of oriented samples and their physical characterization is currently in progress and the results will be reported elsewhere.

---

(43) Belarbi, Z.; Sirlin, C.; Simon, J.; Andre, J.-J. *J. Phys. Chem.* **1989**, *93*, 8105.
(44) Lelievre, D.; Petit, M. A.; Simon, J. *Liq. Cryst.* **1989**, *4*, 707.
(45) Komatsu, T.; Ohta, K.; Watanabe, T.; Ikemoto, H.; Fujimoto, T.; Yamamoto, I. *J. Mater. Chem.* **1994**, *4*, 537.

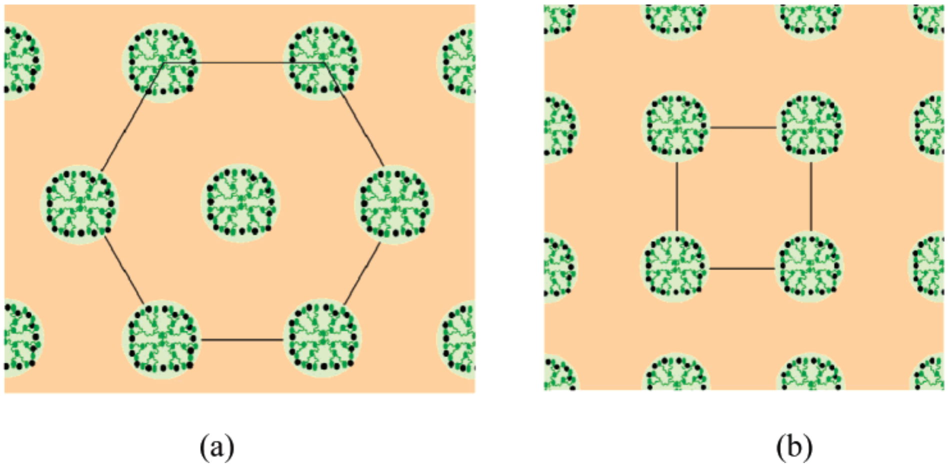

Figure 7. Schematic representation of the molecular organization in a columnar mesophase: (a) hexagonal; (b) tetragonal.

Conclusions

We have described a simple noncovalent dendrimer system which exhibit thermotropic liquid crystal behavior. This system is achieved by converting the dendrimer surface from hydrophilic ($-NH_2$) to hydrophobic (alkyl chains). The method is based on the formation of ion pairs between *n*-alkanoic acids and the terminal amine groups of PAMAM and PPI dendrimers. The ionic dendrimers obtained do not have aromatic (pro)-mesogenic groups in their structure, which indicates that the ionic interaction plays a key role in the formation of a thermotropic lamellar mesophase and the enhancement of the thermal stability. The results reported herein indicate that these systems tend to assemble in smectic LC phases, as happened for covalent LC dendrimers. The exception to this trend is found for PPI-derived dendrimers of the fifth generation, which self-assemble into a columnar supramolecular structure. Finally, these materials are thermally stable at low temperatures (below 100 °C), since over that temperature, the progressive formation of amide bonds occurs, which leads to a decrease of the mesophase temperature interval.

Acknowledgment. This work has been supported by the CICYT of Spain and the FEDER funds (EU) under the projects MAT2002-04118-C02-01 and MAT2003-07806-C01, by the European Union under the RTN Project “Supermolecular Liquid Crystal Dendrimers (LCDD)” (HPRN-CT2000-00016), and by the Diputación General de Aragón. R.M.R. acknowledges a fellowship from the Ministerio de Educación y Ciencia (Spain).

Supporting Information Available: Experimental details, main IR data for ionic PAMAM- and PPI-derived ionic dendrimers (Tables 1 and 2), XRD patterns obtained for the smectic A, hexagonal columnar, and tetragonal columnar mesophases, and the determination of the thickness *h* of one dendrimer along the axis of the column in a columnar phase and of the cross section *s* of one dendrimer in a smectic A mesophase by theoretical calculations starting from the experimentally measured spacings *d* obtained by XRD and the values of molecular weight. This material is available free of charge via the Internet at http://pubs.acs.org.

JA042264H